

Spectrophotometric Investigation and Computational Studies of Zirconium(IV)-3-hydroxy-2-[1'-phenyl-3'-(p-methoxyphenyl)-4'-pyrazolyl]-4*H*-chromen-4-one Complex

Chetna Dhonchak^a, Nivedita Agnihotri^{a, *}, Akshay Kumar^b,
Raj Kamal^c, Abhinav Thakur^d, and Ashish Kumar^d

^a Department of Chemistry, Maharishi Markandeshwar (Deemed to be University),
Mullana, Haryana, Ambala-133207 India

^b Department of Chemistry, Dyal Singh College, Haryana, Karnal-132001 India

^c Department of Chemistry, Kurukshetra University, Haryana, Kurukshetra-136119 India

^d Department of Chemistry, Faculty of Technology and Science,
Lovely Professional University, Punjab, Phagwara-144411 India

*e-mail: nivagni11@gmail.com

Received June 27, 2022; revised September 14, 2022; accepted January 5, 2023

Abstract—A new binary liquid-liquid extraction technique incorporating 3-hydroxy-2-[1'-phenyl-3'-(p-methoxyphenyl)-4'-pyrazolyl]-4*H*-chromen-4-one (HPMPC) has been developed for the trace spectrophotometric detection and determination of Zr(IV). The optimal conditions for the formation of Zr(IV)–HPMPC complex in a ratio of 1 : 3 (M : L) were investigated. The resulting complex has yellow color and allows for the micro level measurement of zirconium in a straightforward and cost-effective manner. The process is quick, sensitive (1.073×10^5 L/mol cm) and selective. A good linearity ($r = 0.9998$) was observed for Zr(IV) in the range of 0.20–0.8 µg/mL. The approach is extremely repeatable with acceptable precision and accuracy (RSD of 0.3%) and can be expanded to include the examination of zirconium in a variety of samples (synthetic, natural and technical). The analytical investigation was successfully extended to DFT calculations to forecast the structural geometry and confirm the complex ultimate stoichiometry. The calculations not only produced an optimal complex structure, but also confirmed the bidentate ligand chelating efficacy by coordinating benzopyran ring to the metal center.

Keywords: zirconium, 3-hydroxy-2-[1'-phenyl-3'-(p-methoxyphenyl)-4'-pyrazolyl]-4*H*-chromen-4-one, extraction, chloroform, spectrophotometric determination, DFT

DOI: 10.1134/S1061934823070055

The most economic sources of zirconium are zirconium silicate (ZrSiO₄) and baddeleyite (ZrO₂). Zr(IV) is employed in the production of water repellent fabrics, dye pigments, optical glasses with high refractive index, ceramics, nuclear and pigment industries due to its hardness, transparency and ability to increase corrosion resistance and mechanical strength. Surgical tools, photoflash bulbs, explosive primers, rayon spinnerets and lamp filaments employ the metal as an alloying element [1–3]. Because of its bio-inert non-restorative properties, zirconium oxide is used in medical fields and dentistry materials [4, 5]. As a result, reliable and specific detection of zirconium in environmental, biological and industrial materials is required.

First derivative spectrophotometry, graphite furnace atomic absorption spectrometry, inductively coupled plasma atomic emission spectrometry, laser ablation inductively coupled plasma optical emission

spectrometry, X-ray spectrometry, potentiometry, optical sensor, reversed phase liquid chromatography and UV-Vis spectrophotometry have been reported for analytical determination of zirconium [1, 2, 6–16]. The most significant disadvantage of most of the mentioned techniques is the high cost of service and requirement of qualified personnel; however, UV-Vis spectrophotometric methods of determination require cheap instrumentation, and the technique is easy to learn. There have been reports of many spectrophotometric methods for determining Zr(IV) using various reagents [1, 2, 17–23] including the techniques with higher molar absorption coefficients and lower detection limits for zirconium [22, 23]. The limitations of these methods are decreased stability, sensitivity and selectivity that can be satisfactorily compared to the proposed method [1, 2, 17–23].

In the present communication, spectrophotometric determination of Zr(IV) as its 3-hydroxy-2-[1'-phenyl-

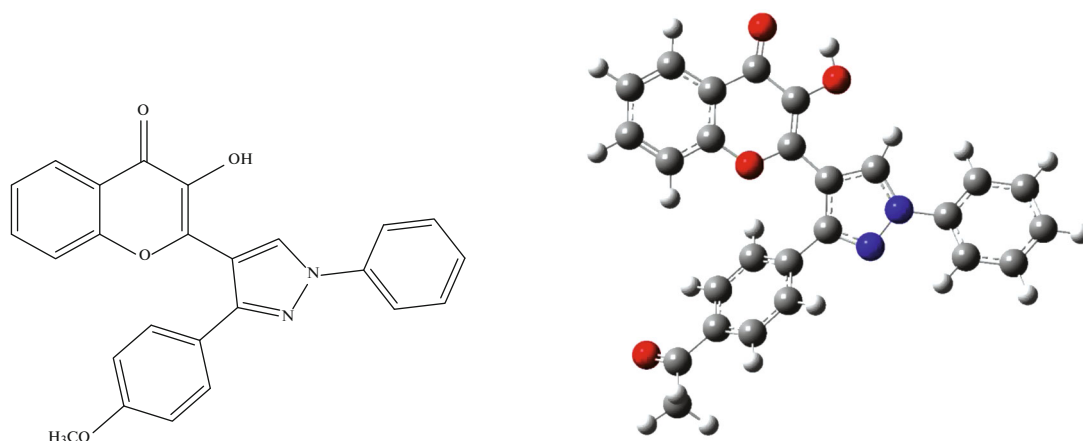


Fig. 1. Structure of HPMPC.

3'-(p-methoxyphenyl)-4'-pyrazolyl]-4*H*-chromen-4-one (HPMPC) complex has been carried out to establish its optimum conditions. Sensitivity and selectivity of the system were beneficial. Along with photometric investigation, computational methods were also executed showing consistency in results with the spectrophotometric data.

EXPERIMENTAL

Apparatus, reagents and solutions. A UV-Vis spectrophotometer (2375; Electronics India) with 10 mm matched quartz cells was used for ocular scanning. For analytical investigations, 1 mg/mL stock solution of Zr(IV) was attained by dissolution of promptly weighed amount of $\text{ZrOCl}_2 \cdot 8\text{H}_2\text{O}$ (CDH® “AR”) in 2 M solution of HCl and making the volume to the mark in a 100 mL volumetric flask prior to its standardization gravimetrically. Chloroform (CDH® “AR”) was distilled, and the fraction distilling at 60–61°C was used for extraction. 3-Hydroxy-2-[1'-phenyl-3'-(p-methoxyphenyl)-4'-pyrazolyl]-4*H*-chromen-4-one (Fig. 1, molar weight of 410 g/mol, melting point of 202–204°C) was synthesized as per the reported method [24–27], and its 0.1% (w/v) prepared fresh solution in ethanol was used for complexation.

Synthetic and technical specimens. The formed yellow colored complex was checked for selectivity through analysis of various samples prepared by mixing different metal ions in the desired proportions as shown in Table 1. As per earlier outlined work, reverberatory flue dust and water samples (tap and well) were prepared, and a suitable specimen of each was taken for zirconium determination as described in the present methodology [21].

Quantum chemical/density functional theory (DFT) calculation details. Density functional theory and theoretical calculations for the ligand (HPMPC) and Zr(IV)-HPMPC complex were carried out using Gaussian09 package [28]. For HPMPC, basis set used

was B3LYP, 6-311G, ++, d, p, Charge 0 with singlet spin, while in case of Zr(IV)–HPMPC complex, optimization basis set of B3LYP, LanL2DZ, Charge 0 with singlet spin was used [29]. Quantum chemical parameters like highest occupied molecular orbital energy (HOMO) and lowest unoccupied molecular orbital energy (LUMO), HOMO-LUMO energy gap (ΔE_{gap}) and other reactivity descriptors were calculated for better structural understanding of HPMPC and its Zr(IV) complex as is used in the earlier studies [30].

Extraction of complex. ≤ 8 μg of Zr(IV) solution was taken along with 0.8 mL of 0.1% (w/v) HPMPC ethanolic solution maintained at pH 3.82 in a 125 mL separating funnel, consequently making its final aqueous volume to 10 mL using distilled water. The aqueous content so formed was equilibrated for 30 s after the addition of equal volume of chloroform releasing the pressure recurrently through the stopcock. After phase separation, the yellow complex in the organic layer was collected in a 10 mL volumetric flask by passing through a Whatman filter paper no. 41 (pretreated with chloroform) and making the volume to the mark with pure chloroform. Absorbance of the yellow colored extract was measured at 420 nm against reagent blank prepared under similar conditions. After maintaining the optimum conditions for the suggested method, the amount of zirconium was determined from the standard curve plotted between different Zr(IV) amounts and corresponding absorbance values.

Modifications for the samples containing W(VI), Nb(V) and Fe(III). For each of 0.5 mg of W(VI) and Nb(V), 50 mg of sodium potassium tartrate and 100 mg of ascorbic acid for 0.5 mg of Fe(III) were added as masking agents prior to the addition of HPMPC in a 10 mL aqueous solution.

Table 1. Analysis of various synthetic and technical samples

Sample composition		Zr(IV) found, $\mu\text{g}/10\text{ mL}^b$
matrix ^a	Zr(IV) added, $\mu\text{g}/10\text{ mL}$	
Zn(1), Hg(5), Cr ^{VI} (2)	4.00	4.02 ± 0.01
Fe ^{III} (0.5), Co(5), Se(2) ^c	5.00	4.90 ± 0.08
Pd(0.5), Al(5), Ni(2)	8.00	7.94 ± 0.02
Fe ^{II} (0.2), Nb(0.2), As(0.5) ^d	4.00	3.99 ± 0.01
Ba(5), Sr(0.5), Ir(5)	7.00	7.16 ± 0.01
Pd(0.5), Cu(2), Bi(0.5)	5.00	5.03 ± 0.01
Ti(0.5), Ir(5), Hg(5)	4.00	3.98 ± 0.01
Au(0.5), Ru(5), Pt(0.5)	7.00	6.98 ± 0.01
Mg(5), Sn(0.5), W(0.05) ^d	5.00	5.02 ± 0.02
Ni(2), Al(5), Bi(0.5)	7.00	7.13 ± 0.05
Ni(0.07), W(0.123) ^{d, e}	5.00	5.03 ± 0.02
Ni(2.68) ^e	5.00	4.99 ± 0.01
Tap water	4.00	3.99 ± 0.01
Ground water	5.00	5.03 ± 0.02
Reverberatory flue dust	4.00	4.08 ± 0.05

^aFigure in parentheses indicates amount of metal ion in mg per 10 mL, ^b average of triplicate analysis \pm SD, ^c in the presence of 100 mg of ascorbic acid, ^d in the presence of 50 mg of sodium potassium tartarate, ^e composition analogous to cooperite and nickel zirconium, respectively.

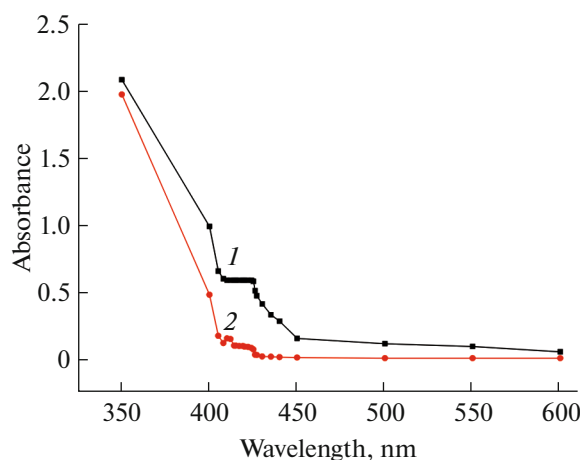


Fig. 2. Dependence of optical density of Zr(IV)–HPMPC complex in chloroform on wavelength: (1) complex measured against reagent blank; (2) reagent blank measured against chloroform; 0.5 $\mu\text{g}/\text{mL}$ Zr(IV), other conditions as cited in procedure.

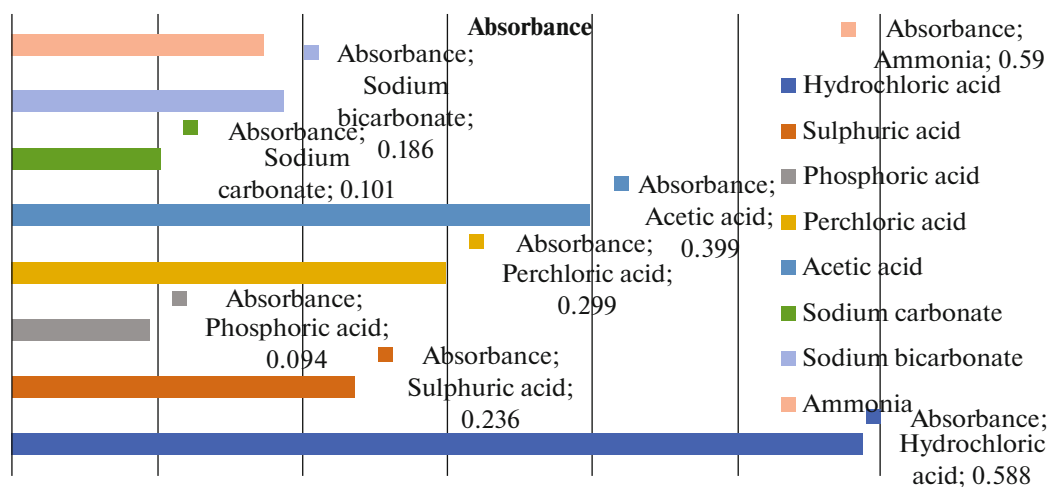


Fig. 3. Effect of media on Zr(IV)–HPMPC complex.

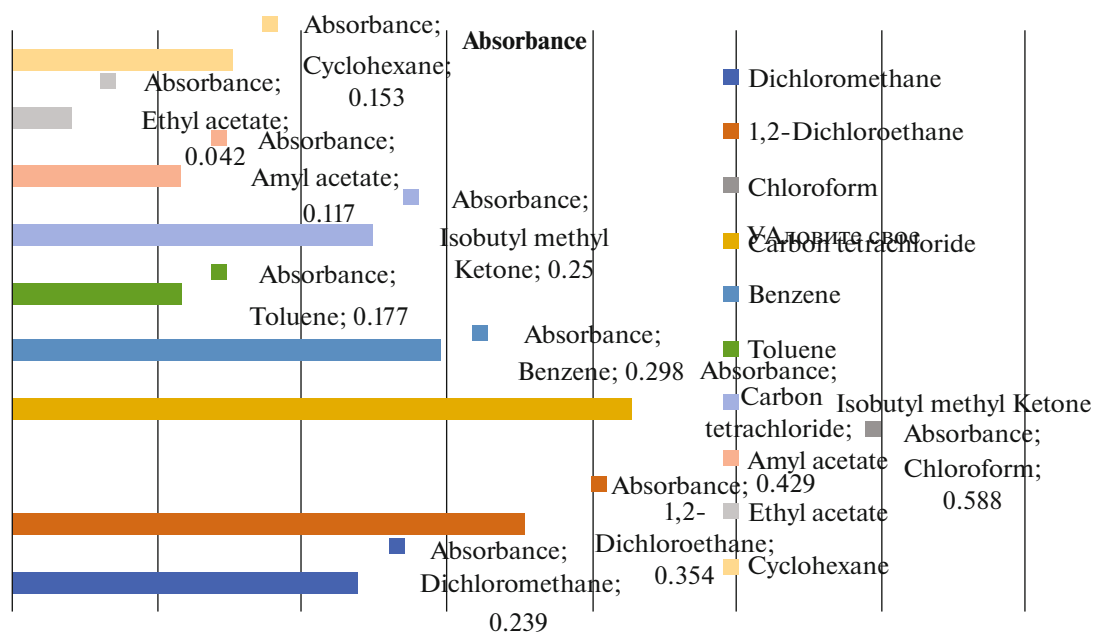


Fig. 4. Effect of solvents on Zr(IV)–HPMPC complex.

RESULTS AND DISCUSSION

Dependence of optical density on wavelength.

HPMPC was proven to be a very good complexing agent, reacting with zirconium in tetravalent state forming a yellow stable (holding a stability up to 3 days) and highly sensitive ($\epsilon = 1.073 \times 10^5$ L/mol cm) binary complex in HCl medium (pH 3.63–4.28). Figure 2 depicts the dependence of optical density for Zr(IV)–HPMPC complex showing maximum and constant absorption range of 410–424 nm in comparison to blank prepared analogously, where a working wavelength of 420 nm was taken.

Variation of medium and solvent. Different media tested to achieve maximum and constant absorbance are summarized in Fig. 3. Although maximum absorbance was observed both in ammonia as well as hydrochloric acid media, HCl was preferred as a complexing medium due to stability reasons. When ammonia was used as a medium for complexation, the complex was not found stable even for a minute showing continuous fall in absorbance.

Figure 4 depicts the extraction of Zr(IV)–HPMPC complex in different solvents. More than 95% extraction giving maximum absorbance of the complex was noted in chloroform, and hence it was chosen for further studies.

Effect of pH, reagent concentration and equilibration time. The influence of various parameters including pH (using hydrochloric acid), HPMPC concentration and equilibration time on Zr(IV)–HPMPC extraction and determination process is given below:

2 M HCl, mL	0.00	0.04	0.08	0.10	0.12–0.24	0.26	0.28	0.32	0.36	0.40
pH	4.99	4.79	4.54	4.41	4.28–3.63	3.49	3.35	3.13	2.95	2.70
Absorbance	0.039	0.347	0.452	0.510	0.588	0.518	0.450	0.398	0.351	0.212

(Conditions: 5 µg of Zr(IV), variable pH, 1 mL of 0.1% (w/v) HPMPC in ethanol, aqueous and solvent (chloroform) volumes of 10 mL, equilibration time of 30 s, λ_{\max} of 420 nm.)

HMTC, mL	0.0	0.2	0.4	0.6	0.7–1.1	1.2	1.3	1.4
Absorbance	0.007	0.230	0.340	0.447	0.588	0.480	0.243	0.134

(Conditions: pH 3.82, remaining parameters were the same as in the previous data except variation in HPMPC concentration.)

Equilibration time, s	0	2	5	10	15–300
Absorbance	0.009	0.159	0.510	0.535	0.588

(Conditions: 0.8 mL of 0.1% (w/v) HPMPC in ethanol, remaining conditions were the same as in the previous data except variation in equilibration time.)

Effect of anions/complexing agent and cations. To study the selectivity and tolerance limit of Zr(IV)–HPMPC complex, effect of diverse anions/complexing agents and cations was studied by their addition

(before addition of the reagent) under similar conditions of the recommended procedure of determination, which is summarized in Tables 2 and 3, respectively. Among numerous foreign ions studied, oxalate,

Table 2. Effect of anions/complexing agents on Zr(IV)–HPMPC complex

Anion/complexing agent	Tolerance limit, mg/10 mL	Absorbance
None	–	0.588
Sodium chloride, sodium bromide, potassium iodide, potassium fluoride, sodium sulphate, sodium nitrite sodium carbonate, sodium sulphite, thiourea, sulfosalicylic acid, ascorbic acid, hydrazine sulphate, potassium thiocyanate	100	0.588
Sodium acetate, sodium potassium tartrate	50	0.588
Disodium EDTA, sodium phosphate, sodium dithionite	20	0.588
Hydrogen peroxide (30%), glycerol	1 ^a	0.588
Sodium nitrate ^b	0.1	0.215
Sodium oxalate ^b	0.1	>2

^a Amount added in mL, ^b seriously interfered.

Table 3. Effect of cations on Zr(IV)–HPMPC complex

Cation ^a	Tolerance limit, mg/10 mL	Absorbance
None	–	0.588
Ce(IV), Ir(III), Ru(III), Al(III), Pb(II), Hg(II), Ba(II), Co(II), Mg(II), Mn(II), Cd(II), Zn(II), Ni(II)	10	0.588
Cr(VI), Se(IV), Cu(II), Ca(II), Ag(I)	5	0.588
Pt(IV), Ti(IV), Au(III), Cr(III), As(III), Bi(III), Cu(II), Sr(II), Pd(II), Sn(II), Fe(II)	1	0.588
W(VI) ^b , Nb(V) ^b , Fe(III) ^c	0.5	0.588
Mo(VI), La(III)	0.2	0.588
V(V) ^d	0.1	>2.000

^a Initial oxidation state is shown in parentheses, ^b in the presence of 50 mg of sodium potassium tartrate, ^c in the presence of 100 mg of ascorbic acid, ^dinterfered seriously.

Table 4. Spectrophotometric and statistical data

Parameter	Value
λ_{\max} , nm	410–424
Optimum range of determination, ppm	0.20–0.8
Molar absorptivity, L/mol cm	1.073×10^5
Sandell's sensitivity, $\mu\text{g}/\text{cm}^2$	0.00085
Correlation coefficient (r)	0.9998
Regression equation ^a	$y = 1.2046x - 0.0137$
Standard deviation	± 0.0016
Relative standard deviation, %	0.3
Limit of detection, $\mu\text{g}/\text{mL}$	0.01

^a $y = bx + a$, where y is absorbance, x is Zr(IV) concentration in $\mu\text{g}/\text{mL}$.

nitrate and V(V) interfered seriously even in traces with the presented extraction determination of Zr(IV).

Spectrophotometric and statistical specifics. Zr(IV)–HPMPC complex in adherence to the procedure showed linear response in the range of 0.20–0.8 ppm of Zr(IV) by Ringbom plot. The correlation coefficient of 0.9998 further confirmed linearity for the procedure. Spectral and statistical attributes are summarized in Table 4.

Stoichiometry of the complex. Stoichiometric ratio of Zr(IV)–HPMPC complex as 1 : 3 was established and confirmed by Job's continuous variations method revised for a two-phase system by Vosburgh and Cooper, mole ratio method and equilibrium shift methods [31].

Obtained from above stoichiometry, Fig. 5 shows the probable and optimized structures for Zr(IV)–HPMPC complex.

Geometrical optimization of ligand and complex using density functional theory. *Highest occupied and unoccupied molecular orbital energies.* Computational studies have offered a great scope to generate optimal geometry structures and electronic properties of the ligands and their respective complexes [32]. To analyze stability and reactivity features of HPMPC and its Zr(IV) complex, DFT study was carried out.

The electron density distributions of the frontier molecular orbitals (FMOs), namely, the highest occupied molecular orbitals and lowest unoccupied molecular orbitals, are depicted in Figs. 6 and 7 for HPMPC and its Zr(IV) complex, respectively.

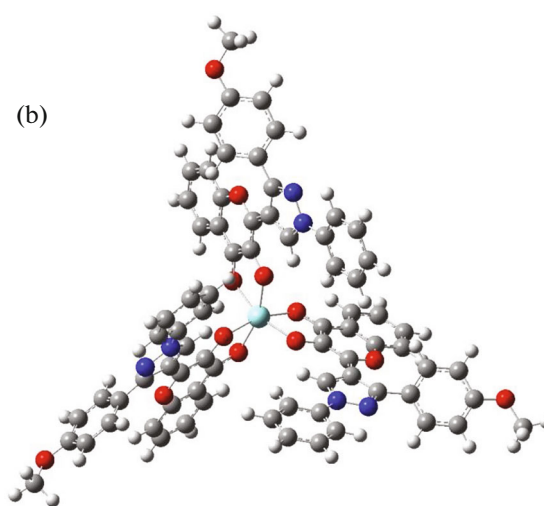
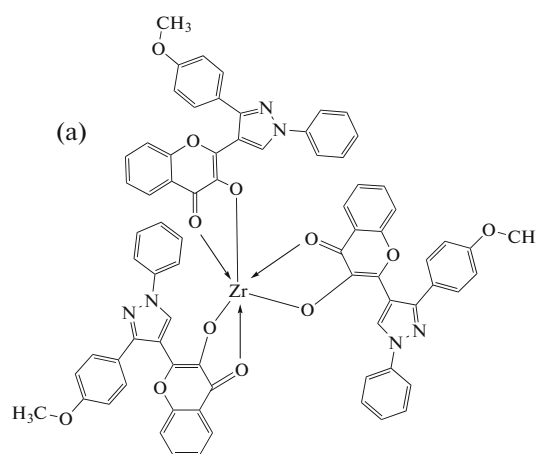


Fig. 5. (a) Proposed and (b) optimized structure of Zr(IV)–HPMPC complex.

E_{HOMO} and E_{LUMO} are commonly used as indices of reactivity of a molecule in terms of its willingness to donate and receive electron(s) under favorable conditions, respectively. The energy difference between HOMO and LUMO or frontier orbital gap or ΔE_{gap} is a key factor in determining electrical transport attribute of a molecule. Table 5 enlists the FMO energies, ΔE_{gap} and dipole moments of examined Zr(IV)–HPMPC complex. HPMPC molecule with a small ΔE_{gap} is highly polarizable, has a high chemical

Table 5. Quantum chemical parameters

Compound	HOMO, eV	LUMO, eV	ΔE_{gap} , eV	Dipole moment (Debye)	Predicted energy change (Hartree)
HPMPC ligand	−3.23489	−2.75216	0.48273	1.354262	-9.54×10^{-9}
Zr(IV)–HPMPC complex	−6.15793	−2.30834	3.84959	4.041696	-3.91×10^{-9}

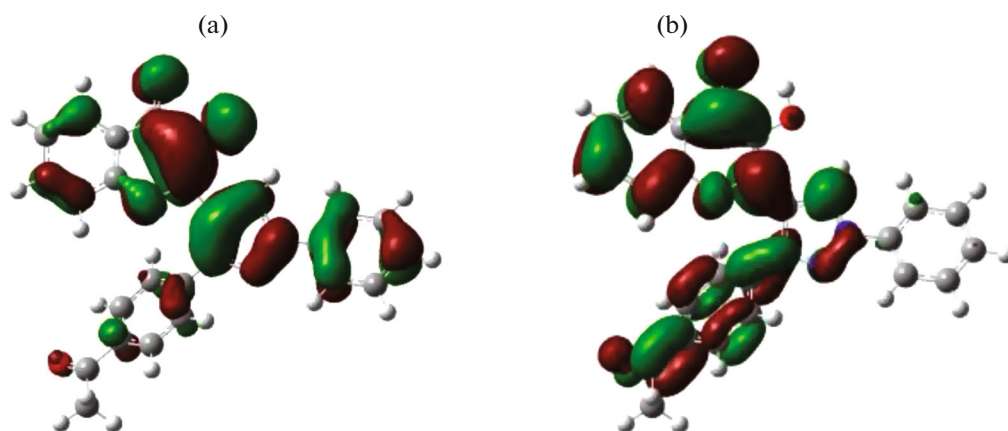


Fig. 6. (a) Highest occupied molecular orbital and (b) lowest unoccupied molecular orbital of HPMPC.

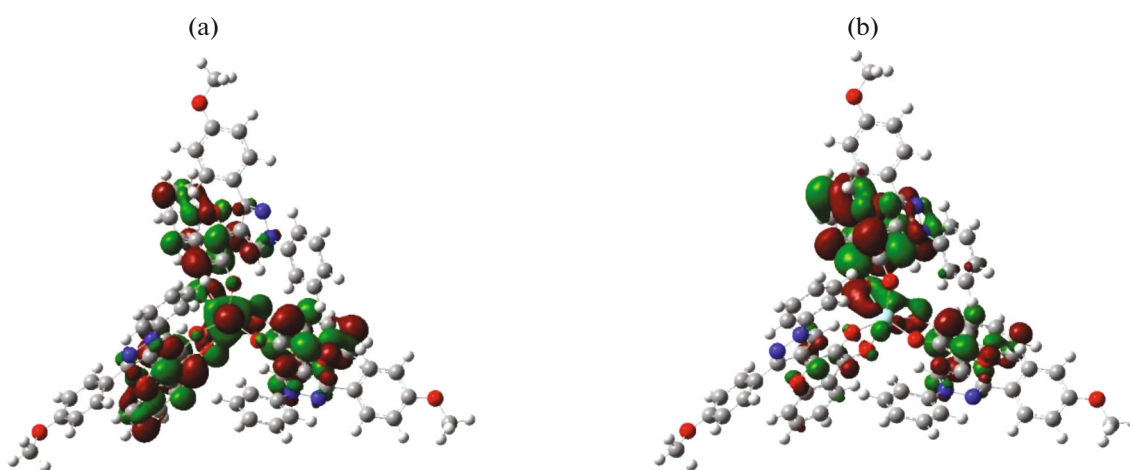


Fig. 7. (a) Highest occupied molecular orbital and (b) lowest unoccupied molecular orbital of Zr(IV)-HPMPC complex.

reactivity, a low kinetic stability and is referred to as a soft molecule. Hence, we can infer that ligand HPMPC acting as a chelating agent is donating its electron density from its HOMO to LUMO of central metal ion, Zr(IV), for chelation. Zr(IV)-HPMPC complex thus formed after complexation has high value of ΔE_{gap} , which suggests and supports its stability in accordance to spectrophotometric analysis. Further, HPMPC complex of Zr(IV) has high value of dipole moment indicating strong dipole-dipole interactions which can be extended to its application in biological systems [33, 34]. Predicted energy change is the asserted energy change that a molecule may attain for the optimized structure with no negative frequencies for the subsequent evaluation of the HOMO and LUMO structures along with the acquired values and is represented in Table 5 [35].

Reactivity descriptors. Reactivity descriptors such as chemical potential (P_i), absolute electronegativities (χ), absolute hardness (η), global electrophilicity (ω),

absolute softness (σ) and fraction of electrons transferred (ΔN) were estimated for both HPMPC and its Zr(IV) complex using Eqs. (1)–(6) [36–39]:

$$X = -(E_{\text{LUMO}} + E_{\text{HOMO}})/2, \quad (1)$$

$$\eta = (E_{\text{LUMO}} - E_{\text{HOMO}})/2, \quad (2)$$

Table 6. Calculated reactivity descriptors

Parameter	HPMPC	Zr(IV)-HPMPC complex
χ , eV	2.9935	4.2331
η , eV	0.2414	1.9248
σ , eV ⁻¹	4.1425	0.5195
P_i , eV	-2.9935	-4.2331
ω , eV	4.3264	4.6549
ΔN	12.4006	2.1993

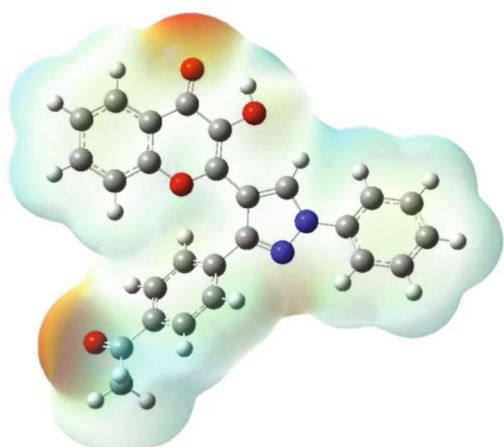


Fig. 8. Electrostatic surface potential of HPMPC.

$$\sigma = 1/\eta, \quad (3)$$

$$P_i = -\chi, \quad (4)$$

$$\omega = P_i^2/2\eta, \quad (5)$$

$$\Delta N = -P_i/\eta. \quad (6)$$

The following interpretations can be modelled from data in Table 6: first, positive high value of electronegativity (χ) for Zr(IV)–HPMPC complex sug-

gests electrons acceptance by Zr(IV) from its ligand environment indicating a decrease in its energy and thus greater stability of the formed complex; second; absolute hardness (η) and absolute softness (σ), respectively denoted by high and low ΔE_{gap} , show HPMPC as a soft molecule and Zr(IV)–HPMPC complex as the hard one justifying more reactivity of ligand and thus the formation of a stable and soft complex with low reactivity; third; work function (P_i) has larger negative value for Zr(IV) HPMPC complex indicating its greater stability and its unwillingness to undergo decomposition into its constituent metal ion and ligand, respectively; fourth; electrophilicity index (ω) is the measure of the propensity of a species for its electron acceptance. High nucleophilicity and electrophilicity of compounds correspond to opposite ends of the scale of global reactivity indices, according to Domingo et al. [40]. A good, more reactive nucleophile has a lower value of ω ; a good electrophile, on the other hand, has a high value of ω . Lower ω value for the ligand indicates its nucleophilic behavior thus favoring its complexation with positively charged Zr(IV) ion; fifth, ΔN or the fraction of electrons transferred is high for HPMPC further giving grounds for electron donation/transfer from ligand to tetravalent zirconium metal.

Electrostatic surface potential. The electrostatic surface potential (ESP) is a valuable approach for detecting a molecule reactivity as well as the presence of

Table 7. Comparison of the proposed method with existing ones

Aqueous condition	λ_{max} , nm	Molar absorption coefficient, L/mol cm	Interference	Reference
Zr(IV), Mordant blue 2RL, 2 M HCl	583	4.93×10^3	–	[1]
Zr(IV) and 4-chloro-N-(2,6-dimethylphenyl)-2-hydroxy-5-sulfamoylbenzamide (xipamide), pH 2.0–12.0 in HCl medium	333	5.6×10^4	–	[2]
Zirconium(IV), 5,7-dibromo-8 hydroxyquinoline, 1 M HCl	416	1.05×10^5	Ti(IV), V(V), oxalate, fluoride, EDTA disodium salt	[17]
Zr(IV), albendazole	555	0.8350×10^4	–	[18]
Zr(IV), Xylenol Orange	–	–	Fluoride	[19]
Zr(IV), 6-chloro-3-hydroxy-2-(2'-hydroxyphenyl)-4-oxo-4H-1-benzopyran (CHHPB), propan-1-ol-H ₂ O	400	1.780×10^4	Nb(V), Pb(II), EDTA disodium salt, tartrate, oxalate, phosphate	[20]
Zirconium(IV), 3-hydroxy-2-[2'-(5'-methylthienyl)]-4H-chromen-4-one (HMTc), pH 7.05–7.09	430	8.22×10^4	None	[21]
Zr(IV), Chrome Azurol S (CAS), pH 4.2	498	3.93×10^3	–	[22]
Zr(IV), arsenazo III (1,8-dihydroxynaphthalene-3,6-disulphonic acid-2,7-bis[(azo2)-phenylarsonic acid]), 0.2–10 M HCl	–	–	Th(IV)	[23]
Zr(IV), 3-hydroxy-2-[1'-phenyl-3'-(p-methoxyphenyl)-4'-pyrazolyl]-4H-chromen-4-one (HPMPC), pH 3.63–4.28	420	1.073×10^5	V(V), oxalate, nitrate	Proposed method

inter or intramolecular interactions in the molecule [41, 42]. This presentation also helps us in understanding size, site of reactivity, shape and delocalization of charge density of the molecule. Different colors such as yellow, orange, red, bluish green and blue can be used to depict the various regions of electrical potential that appeared at the surface of molecule (HPMPC) in the presented ESP diagrams.

Figure 8 shows the plot of ESP of HPMPC molecule using color code in the range of -5.128×10^{-2} to $+5.128 \times 10^{-2}$. The electron-rich area or a more negative site is shown by red, whereas the positive site is represented by blue. In the HPMPC molecule, the highest electron density is majorly distributed over pyran ring suggesting it to be the donor site. This conclusion is in accordance with the structure deduced by Job's continuous variation method, mole ratio method and equilibrium shift methods.

CONCLUSIONS

3-Hydroxy-2-[1'-phenyl-3'-(p-methoxyphenyl)-4'-pyrazolyl]-4*H*-chromen-4-one-zirconium(IV) complex was investigated and subjected to analytical and computational studies. Micro determination of the yellow colored complex was carried out evaluating stoichiometric ratio of 1 : 3 (M : L) in hydrochloric acid medium sustained at pH 3.63–4.28, extracted into chloroform manifesting maximum and stable color intensity in the wavelength range of 410–424 nm. Strict adherence to Beer's law was observed for Zr(IV) with an optimum range of determination as 0.20–0.8 ppm Zr(IV) per Ringbom plot. The molar absorption coefficient calculated for the formed complex at 420 nm was 1.073×10^5 L/mol cm. Statistically observed parameters include linear regression equation of $y = 1.2046x - 0.0137$, correlation coefficient of 0.9998 and detection limit of 0.01 $\mu\text{g/mL}$ of the suggested procedure. Density functional theory was successfully applied for supplementing the results obtained via spectrophotometric determination. The offered procedure holds satisfactory comparison with several existing methods of zirconium determination as is mentioned in Table 7 [1, 2, 17–23] and has been utilized in various synthetic, natural and industrial samples adequately.

ACKNOWLEDGMENTS

The authors are sincerely thankful to the authorities, Maharishi Markandeshwar (Deemed to be University), Mullana.

CONFLICT OF INTEREST

No conflicts of interest is declared by the authors.

REFERENCES

- Hamed, M.M. and Aglan, R.F., *Microchem. J.*, 2019, vol. 149, p. 104032. <https://doi.org/10.1016/j.microc.2019.104032>
- Al-Kady, A.S., *Spectrochim. Acta, Part A*, 2012, vol. 97, p. 284. <https://doi.org/10.1016/j.saa.2012.06.019>
- Loh, H.C., Ng, S.M., Ahmad, M., and Taib, M.N., *Anal. Lett.*, 2005, vol. 38, no. 8, p. 1305. <https://doi.org/10.1081/AL-200060968>
- Bagd, E. and Tuzen, M., *RSC Adv.*, 2015, vol. 5, p. 107872. <https://doi.org/10.1039/C5RA21267G>
- Afzali, D., Fathirad, F., Ghaseminezhad, S., and Afzali, Z., *Environ. Monit. Assess.*, 2014, vol. 186, no. 6, p. 3523. <https://doi.org/10.1007/s10661-014-3635-7>
- El-Sayed, A.A., Hamed, M.M., and El-Reefy, S.A., *J. Anal. Chem.*, 2010, vol. 65, no. 11, p. 1113. <https://doi.org/10.1134/S1061934810110043>
- Varghese, A. and George, L., *Spectrochim. Acta, Part A*, 2012, vol. 95, p. 46. <https://doi.org/10.1016/j.saa.2012.04.092>
- Agrawal, Y.K., Sanyal, M., Shrivastav, P., and Menon, S.K., *Talanta*, 1998, vol. 46, no. 5, p. 1041. [https://doi.org/10.1016/S0039-9140\(97\)00383-4](https://doi.org/10.1016/S0039-9140(97)00383-4)
- Faghihian, H. and Kabiri-Tadi, M., *Microchim. Acta*, 2010, vol. 168, nos. 1–2, p. 147. <https://doi.org/10.1007/s00604-009-0273-9>
- Schenk, E.R. and Almirall, J.R., *Forensic Sci. Int.*, 2012, vol. 217, nos. 1–3, p. 222. <https://doi.org/10.1016/j.forsciint.2011.11.009>
- Afzal, M., Hanif, J., Hanif, I., Oadeer, R., and Saleem, M., *J. Radioanal. Nucl. Chem.*, 1990, vol. 139, p. 203.
- Arida, H.A., *Talanta*, 2008, vol. 76, no. 1, p. 40. <https://doi.org/10.1016/j.talanta.2008.01.061>
- Gupta, V.K., Goyal, R.N., and Sharma, R.A., *Int. J. Electrochem. Sci.*, 2009, vol. 4, p. 156.
- Abbaspour, A. and Baramakeh, L., *Sens. Actuators, B*, 2006, vol. 114, no. 2, p. 950. <https://doi.org/10.1016/j.snb.2005.08.044>
- Oszwałdowski, S. and Jakubowska, J., *Talanta*, 2003, vol. 60, no. 4, p. 643. [https://doi.org/10.1016/S0039-9140\(03\)00041-9](https://doi.org/10.1016/S0039-9140(03)00041-9)
- Lasheen, T.A., Hussein, G.M., Khawassek, Y.M., and Cheira, M.F., *Anal. Chem. Indian J.*, 2013, vol. 12, no. 10, p. 368.
- Jain, A., Prakash, O., and Kakkar, L.R., *J. Anal. Chem.*, 2010, vol. 65, no. 8, p. 820. <https://doi.org/10.1134/S1061934810080101>
- El-Shwiniy, W.H., El-Desoky, S.I., Alrabie, A., and Abd El-wahaab, B., *Spectrochim. Acta, Part A*, 2022, vol. 279, p. 121400. <https://doi.org/10.1016/j.saa.2022.121400>
- Prathibha, T., Selvan, B.R., Hemalatha, V., Suba, M.A., Chandra, S., Shaji, D., Vijay, S.K., Sundararajan, K., and Ramanathan, N., *J. Radioanal. Nucl. Chem.*, 2022, vol. 331, no. 5, p. 2383. <https://doi.org/10.1007/s10967-022-08287-0>

20. Chawaria, M. and Sharma, H.K., *Int. J. Green Herbal Chem.*, 2018, vol. 7, p. 230.
<https://doi.org/10.24214/ijghc/gc/7/2/23036>
21. Dhonchak, C., Kaur, N., Agnihotri, R., Berar, U., and Agnihotri, N., in *Mobile Radio Communications and 5G Networks*, Lecture Notes in Networks and Systems, vol. 140, Singapore: Springer, 2020, p. 333.
https://doi.org/10.1007/978-981-15-7130-5_25
22. Ganesh, S., Velavendan. P., Pandey, N.K., Kamachi Mudali, U., and Natarajan, R., *Int. J. Adv. Chem.*, 2014, vol. 2, p. 15.
23. Savvin, S.B., *Talanta*, 1961, vol. 8, p. 673.
[https://doi.org/10.1016/0039-9140\(61\)80164-1](https://doi.org/10.1016/0039-9140(61)80164-1)
24. Algar, J. and Flynn, J.P., *Proc. R. Irish Acad.*, 1934, vol. 42B, p. 1.
25. Oyamada, T., *J. Chem. Soc. Jpn.*, 1934, vol. 55, p. 1256.
26. Prakash, O., Pannu, K., and Kumar, A., *Molecules*, 2006, vol. 11, p. 43.
27. Prakash, O., Kumar, R., and Parkash, V., *Eur. J. Med. Chem.*, 2008, vol. 43, p. 435.
28. Frisch, M.J., Trucks, G.W., Schlegel, H.B., Scuseria, G.E., Robb, M.A., Cheeseman, J.R., Scalmani, G., Barone, V., Mennucci, B., and Petersson, G.A., GAUSSIAN 09, Revision A.02, Gaussian, Inc., Wallingford, CT, 2009.
29. Dennington, R., Keith, T., and Millam, J., GaussView, Version 5, Semichem Inc., Shawnee Mission, KS, 2009.
30. Kumar, A., Trivedi, M., Bhaskaran, Sharma, R.K., and Singh, G., *New J. Chem.*, 2017, vol. 41, p. 8459.
<https://doi.org/10.1039/C7NJ00896A>
31. Tarasiewicz, H.P., Grudiniewska, A., and Tarasiewicz, M., *Anal. Chim. Acta*, 1977, vol. 94, p. 435.
32. Bagheri, H., Saber-Tehrani, M., Shishehbore, M.R., and Shahvazian, M., *Prog. Color Color. Coat.*, 2010, vol. 2, p. 58.
<https://doi.org/10.30509/PCCC.2010.75773>
33. Burke, K., Car, R., and Gebauer, R., *Phys. Rev. Lett.*, 2005, vol. 94, p. 146803.
<https://doi.org/10.1103/PhysRevLett.94.146803>
34. Nandy, A., Duan, C., Taylor, M.G., Liu, F., Steeves, A.H., and Kulik, H.J., *Chem. Rev.*, 2021, vol. 121, p. 9927.
<https://doi.org/10.1021/acs.chemrev.1c00347>
35. Gandhimathi, R., Dheivamalar, S., and Dhanasekara, R., *Eur. Phys. J. Appl. Phys.*, 2015, vol. 69, p. 10202.
<https://doi.org/10.1051/epjap/2014140426>
36. Ekennia, A.C., Osowole., A.A., Olasunkanmi, L.O., Onwudiwe, D.C., Olubiyi, O.O., and Ebenso, E.E., *J. Mol. Struct.*, 2017, vol. 1150, p. 279.
<https://doi.org/10.1016/j.molstruc.2017.08.085>
37. Vektariene, A., Vektaris, G., and Svoboda, J., *Arkivoc*, 2009, vol. 7, no. 7, p. 311.
<https://doi.org/10.3998/ark.5550190.0010.730>
38. Zayed, E.M., El-Samahy, F.A., and Mohamed, G.G., *Appl. Organomet. Chem.*, 2019, vol. 33, no. 15, p. e5065.
<https://doi.org/10.1002/aoc.5065>
39. Mahmoud, W.H., Sayed, F.N., and Mohamed, G.G., *Appl. Organomet. Chem.*, 2016, vol. 30, p. 959.
<https://doi.org/10.1002/aoc.3529>
40. Domingo, L.R., Aurell, M.J., Pérez, P., and Contreras, R., *Tetrahedron*, 2002, vol. 58, no. 22, p. 4417.
[https://doi.org/10.1016/S0040-4020\(02\)00410-6](https://doi.org/10.1016/S0040-4020(02)00410-6)
41. Ibnouf, E.O., Kaiba, A., Geesi, M.H., Alghamdi, A.M., Aldajani, Z.S., Dehbi, O., Guionneau, P., Azzallouh, R., and Riadi, Y., *J. Mol. Struct.*, 2021, vol. 1246, p. 131214.
<https://doi.org/10.1016/j.molstruc.2021.131214>
42. Dhonchak, C., Agnihotri, N., Mohmad, M., Thakur, A., and Kumar, A., *Res. J. Chem. Environ.*, 2022, vol. 26, no. 6, p. 137.